Enhancing Permeability Resistance of Composite Cryogenic Hydrogen Storage for Sustainable Aviation

L. Li[1*], A. Pilkington[1], N. Du[2], W. Qian[3], A. Islam[3], M. Lanzo[4], P. Shabani[4], J. Laliberte[4]

[1] Aerospace Research Centre, National Research Council Canada, Ottawa, Canada

[2] Clean Energy Institute, National Research Council Canada, Ottawa, Canada

[3] Clean Energy Institute, National Research Council Canada, Vancouver, Canada

[4] Department of Mechanical and Aerospace Engineering, Carleton University, Ottawa, Canada

* *Corresponding author (Lucy.li@nrc-cnrc.gc.ca)*

Keywords: *Composites, Permeability, Cryogenic hydrogen storage, Aviation, Sustainability*

1. Abstract

Hydrogen-powered commercial aviation is considered a promising pathway to reduce carbon emissions in the aerospace sector. A key challenge for hydrogen-based aircraft systems is the durability of cryogenic hydrogen storage tanks. This study investigates a carbon-fibre reinforced thermosetting composite material for cryogenic hydrogen storage, focusing on hydrogen permeability and microcracking caused by cryogenic thermal cycling.

This work presents the development of cryogenic thermal cycling and hydrogen permeation test capabilities for composite materials. It also evaluates ultra-thin ply composites and nanomaterial-modified hydrogen barrier technologies designed to improve permeability resistance by blocking hydrogen diffusion pathways in composite cryogenic tanks. High-pressure hydrogen permeation tests were conducted on composite samples subjected to up to 100 cycles of cryogenic conditioning. Microscopy was performed to examine potential microcracking and other damage caused by thermal cycling.

Based on the hydrogen permeability test results, the hydrogen leak rate was estimated for a representative composite cryogenic tank constructed from the investigated material. It indicates that the composite material would readily meet the permeation limits specified in SAE J2579 for onboard hydrogen storage.

2. Introduction

According to the International Energy Agency (IEA), Transport accounts for around 30% of 2024 global energy demand and is responsible for 24% of worldwide energy-related emissions [1]. Hydrogen-powered commercial aviation has the potential to transform the aerospace industry by replacing traditional fossil fuels with zero-emission hydrogen produced from renewable energy sources. Liquid hydrogen (LH_2) storage is a promising solution for aviation due to its high specific energy density and volumetric efficiency. In the space industry, large-scale heavy-duty rockets

primarily utilize liquid hydrogen as their main propellant, leading to significant energy development in recent years. For the aviation industry, one of the major challenges is the long-term durability as cryogenic LH_2 storage and transportation is expected to last 6-8 years initially, with long-term targets extending to 25 years in service as confidence in the technology grows [2].

A light weight onboard storage system is a primary consideration for hydrogen applications in the aerospace industry. Linerless (i.e. Type V) storage tanks made entirely of carbon fibre reinforced polymer (CFRP) represent the next generation of lightweight solution due to the superior specific strength, stiffness, excellent fatigue resistance, and low thermal conductivity of composite materials. NASA cryotank technology demonstrators for space launch vehicles have shown that cryogenic composite tanks offer 30% in weight savings and 25% in cost savings compared to a state-of-the-art aluminum-lithium cryogenic tank [3].

Metallic hydrogen tank material such as austenitic stainless steel offers low diffusivity [4]; however, metals are known to be susceptible to hydrogen embrittlement that can degrade mechanical properties and lead to catastrophic failure [4]. Fibre-reinforced composite materials, although not subjected to hydrogen embrittlement, are prone to microcracking and fibre-matrix debonding under cyclic loading. Several studies found that composites could be damaged at a low stress level in a cryogenic environment [5]-[8], due to thermal stresses arising from thermal contraction mismatch between the fibres and matrix, forming continuous channels for hydrogen gas migration. Cryogenic thermal stresses can increase hydrogen permeability of composite materials by one to two orders of magnitude compared to pristine materials at the ambient conditions [5]. Furthermore, the resin phase often becomes brittle at cryogenic temperatures, reducing fatigue life [6].

Multiple research activities have been conducted to improve the hydrogen permeability resistance of composite tank materials. Thin-ply layers (less than 100 μm thick) [8]-[10] have been shown to enhance gas leak resistance by delaying matrix microcracking and free-edge delamination. The incorporation of two-dimensional nanomaterials, such as graphene oxide or silica nanoparticles, into epoxy matrices can create tortuous diffusion paths and reduce hydrogen permeability by up to 70 % [11].

This work focuses on developing the capability to assess hydrogen permeability resistance of composite tank materials under cryogenic conditions. It also investigates hydrogen barrier concepts aimed at improving the long-term durability of these materials.

3. Experimental

3.1 Hydrogen barrier materials

IM7/5320-1 carbon fibre / epoxy prepreg (Syensqo, USA), an out-of-autoclave composite, was selected as the candidate for hydrogen storage tank material in this study. Three types of hydrogen barrier concepts were investigated for their potential to enhance hydrogen permeation resistance: an ultrathin-ply composite barrier, a thermoplastic (TP) barrier, and a nanofiller-modified thermoplastic barrier containing 50% nanomaterials by weight (TP-nano).

Compared with the regular ply thickness of 0.14 mm, the ultrathin ply, fabricated from the same IM7/5320-1 composite material, had a thickness of 0.07 mm per ply. The TP and TP-nano barrier films were manufactured at the NRC using an internal NRC solvent-based process. The average thicknesses of the TP and TP-nano films are approximately 0.090 mm and 0.061 mm, respectively.

3.2 Composite test samples with integration of hydrogen barriers

Four types of composite samples (see Table 1) were fabricated following an autoclave curing process recommended by the material supplier: a baseline laminate (BL), a laminate with an embedded ultra-thin ply (UT or U) at the mid-plane, a laminate with a TP hydrogen barrier on the surface, and one with TP-nano hydrogen barrier on the surface. As compared with the baseline laminate, the Ultra-thin samples contain one 70 μm ply embedded at the mid-plane, while the TP and TP-nano were co-bonded either with their respective barrier layers on the laminate surface.

These composite panels measuring 30.5 by 35.6 cm (or 12 by 14 in.) were fabricated and subsequently cut using a waterjet into 5.08 by 5.08 cm (or 2 by 2 in.) specimens for permeability testing and 1.27 by 1.27 cm (or 0.5 by 0.5 in.) specimens for microscopic examination.

Table 1 Composite Sample Configurations and Hydrogen Barriers

Sample types	Layup	Hydrogen barrier type	Barrier thickness before cure (μm)	Sample total thickness (mm)
BL	$90/0_2/90_2/0_2/90$	Baseline (no barrier)	N.A.	1.078 ± 0.031
UT/U	$90/0_2/90_u/0_2/90$	Ultra-thin ply embedment	70	0.881 ± 0.026
TP	$90/0_2/90_2/0_2/90/TP$	100% TP on one surface	95 ± 81	1.166 ± 0.048
TP-Nano	$90/0_2/90_2/0_2/90/TP-nano$	TP with 50% nanomaterials by weight on surface	61 ± 13	1.151 ± 0.025

3.3 Cryogenic thermal cycling

An automated test facility was developed at the NRC to enable repeated thermal cycling of samples between liquid nitrogen (LN_2) at around -198 ºC and ambient conditions. The samples (see Fig. 1) were mounted on a sample rack attached to a hydraulic load frame (see Fig. 2). The test samples were periodically immersed in an LN_2 Dewar, a vacuum-insulated vessel used for cryogenic liquid storage and transport. LN_2 was replenished periodically based on the reading of a weighing scale placed beneath the Dewar to help ensure sufficient LN_2 for full immersion of test samples. The readings from a cryogenic thermometer installed inside the Dewar were also taken as a reference. An infrared (IR) camera was used to monitor sample surface temperatures when the samples were exposed to ambient conditions.

Additional measures were implemented to minimize LN_2 loss. A Styrofoam lid in pink was placed over the Dewar when the samples were immersed in LN_2. Similarly, a wood lid in black, controlled by an actuator synchronized with the load frame motions, was used to contain LN_2 during operation.

The test cycle consisted of 15 seconds of LN_2 immersion followed by 2 minutes at ambient conditions. Completing 100 thermal cycles required approximately four hours, during which about 2-2.5 kg of LN_2 was consumed.

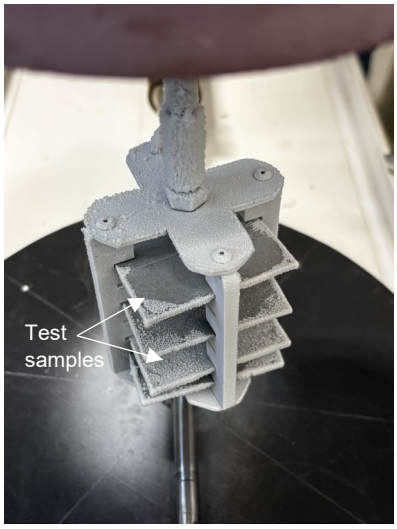

Fig. 1 Sample rack for cryogenic cycling

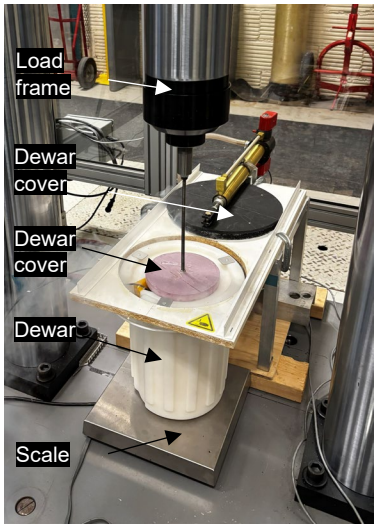

Fig. 2 Automated cryogenic cycling systems

3.4 Permeability rate measurements

Hydrogen permeability is defined as the steady-state volumetric flux of hydrogen gas through a material, normalized for thickness and the applied driving force (often pressure). In this study, an in-house test apparatus was developed to measure hydrogen permeation using a manometric system with a variable pressure upstream and a constant volume downstream chamber, in accordance with ASTM D1434-23 [12].

As illustrated in the schematic of the test rig layout (Fig. 3), a square test specimen measuring 50.8 mm x 50.8 mm (or 2 x 2 in.) was mounted between the upstream reservoir and a calibrated downstream chamber with a volume of 0.01 L, where the permeated hydrogen gas was collected. The effective test area of the test specimen was defined by the inner diameter of the O-ring used in the sealing assembly, which was 50.8 mm (2 in.) in diameter. Prior to testing, the downstream chamber was evacuated to as close to a full vacuum as possible, while the upstream pressure is monitored at a constant 86 psi (5.93 bar).

Permeability was determined by monitoring the downstream pressure increase over time using a Thyracont VCC200MA4 vacuum sensor with a measurement range of 200 to 0.1 mbar. The vacuum pressure measurement has a resolution of 1×10^{-4} mbar. Under steady state conditions, the permeability P depends only on the flow rate of the hydrogen permeating through the composite sample.

Since the facility has not been fully calibrated, the measured results are used primarily for comparative assessment rather than absolute quantification.

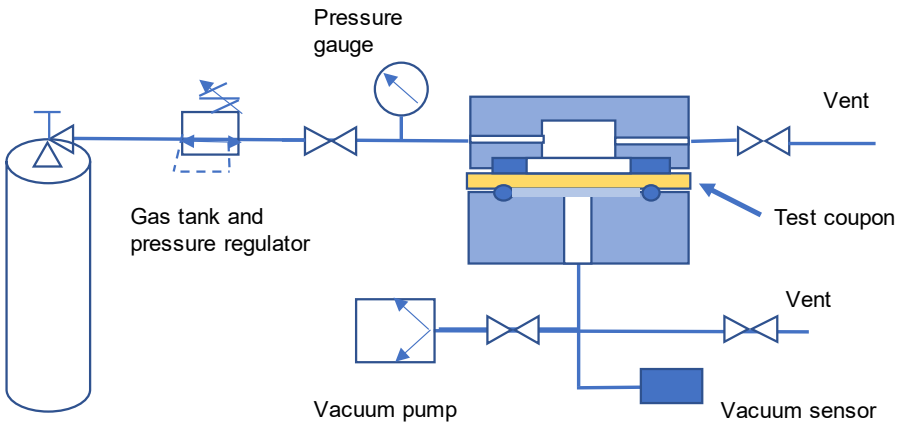

Fig. 3 Schematic of an in-house hydrogen permeation test facility

The gas transmission rate (GTR), in $mol/(m^2\ s\ Pa)$, is calculated from the rate of pressure rise in the downstream chamber over time (see Eqn. 1):

$$\text{GTR} = \frac{V_C}{R\ T\ P_u\ A}\left(\frac{dp}{dt}\right) \qquad \text{Eqn. 1}$$

where, V_c is the volume of the downstream chamber (L), T is the test temperature in (K),

P_u is the pressure of the upstream pressure (Pa), A is the effective area of the test sample in m^2, and dp/dt in Pa/s represents the rate of pressure increase in the downstream chamber. R is universal gas constant, $8.314\ \times 10^3\ (L\ Pa)/(mol\ K)$.

The permeability coefficient P, in $(mol\ m)/(m^2\ s\ Pa)$, is calculated using Eqn. 2.

$$P = GTR\ \times\ l \qquad \text{Eqn. 2}$$

where l is the average thickness of test sample thickness in m.

The permeability coefficient P can be expressed in barrer (in Eqn. 3) where

$$1\ \text{barrer} = 3.349\ \times\ 10^{-16}\frac{mol\ m}{m^2\ s\ Pa} \qquad \text{Eqn. 3}$$

4. Results and Discussions

4.1 Composites surface temperature during cryogenic cyclic testing

During cryogenic thermal cycling, the samples alternated between immersion in liquid nitrogen at approximately -196ºC and exposure to ambient conditions. The temperature inside the LN_2 Dewar was monitored using an ITM traceable cryogenic thermometer (model 98768-60), calibrated over

a range of -200 to 105 ºC (-328 to 221°F). The sample surface temperature under ambient conditions was monitored using a FLIR T540 IR camera, which has a spectral wavelength range of 7.5-14 µm and an accuracy of ±2 % of the reading in its measurement range from -20 to 1500 ºC (-4 to 2732 °F). As shown in Fig. 4, the surface colour appears significantly darker in Cycle 95, as compared with Cycle 2 and 25. This observation corresponds with the visible ice accumulation on the sample surfaces after approximately 50 cycles of cryogenic conditioning. with the measured surface temperature remaining below -70 ºC. It should be noted that the camera readings are only for comparative purposes, as the measured temperature values are not precise.

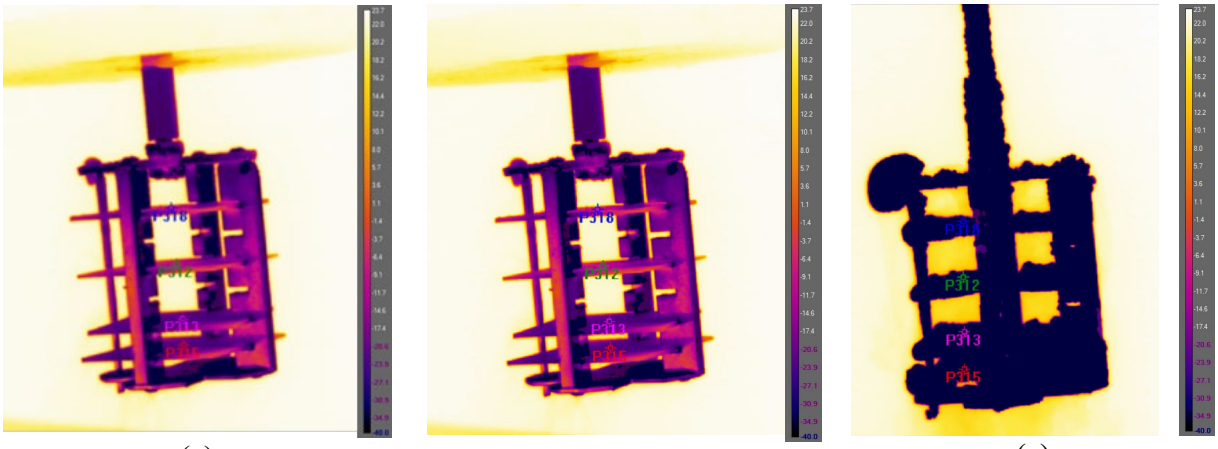

(a) (b) (c)

Fig. 4 IR image of sample surface temperature at the room temperature ambient conditions after (a) 2 cycles, (b) 25 cycles, and (c) 95 cycles during cryogenic thermal cycling

4.2 Effect of cryogenic thermal cycling on composite and hydrogen barrier materials

4.2.1 Microscopy of sample surfaces

The test samples were examined for possible damage using Nikon Eclipse L-150 microscope, which provides image resolution of up to 100 nm. Fig. 5 shows representative microscopy images of the surfaces of the composite (a), TP (b), and TP-nano (c) samples after cryogenic thermal cycling.

No observable surface changes were detected on the composite samples after cryogenic thermal cycling. However, compared with the as-manufactured TP-coated samples, lines of cracking were observed on the thin TP coating after conditioning. This behaviour is likely due to the relatively low fracture toughness, or increased brittleness, of the thermoplastic material under cryogenic conditions.

In contrast, the TP-nano samples, which contain distinct nanomaterial inclusions, did not show visible cracks after repeated exposure to cryogenic conditions. This suggests that the material containing 50% nanomaterials by weight may exhibit improved fracture toughness under cryogenic conditions. Overall, the observations indicate that nanomaterial integration may enhance fracture resistance at cryogenic temperatures. Further work is required to validate these findings

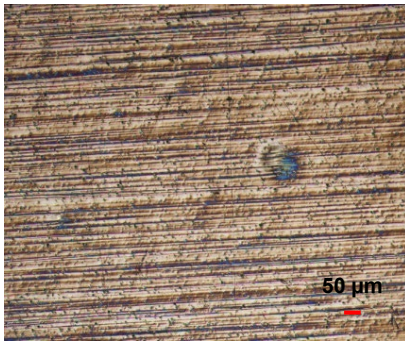

(a) Composite laminate, after 100 cycles

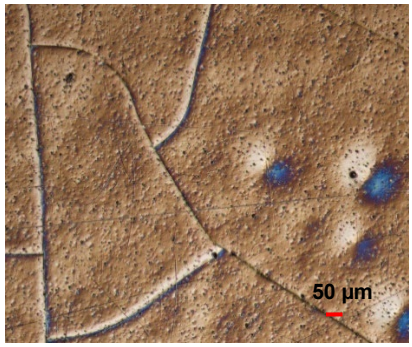

(b) TP hydrogen barrier coating, 100 cycles

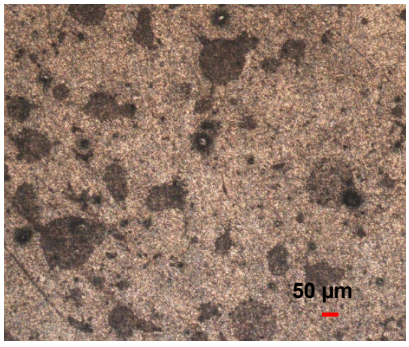

(c) TP-Nano coating with 50% nanomaterials in dark brown, 100 cycles

Fig. 5: Microscopy images of composite samples after 100 cycles of cryogenic conditioning

4.2.2 Effect of cryogenic thermal cycling on composite matrix cracking

The microscopy images of the cross-sections of the composite samples are shown in Fig. 6, including the as-made sample (b) and the samples after cryogenic thermal conditioning (c-f), taken from the location as shown in (a). Images were also taken from other locations. The findings are consistent regardless of locations. Cryogenic exposure was expected to induce matrix cracking in the composite due to high thermal stresses, particularly in the cross-ply layup used in this study. However, no observable matrix cracking was detected in the matrix phase or at the fibre/matrix interface in any of the tested samples.

In this study, no active heating was applied to the samples during the ambient phase of the thermal cycling. As a result, ice accumulated on the sample surfaces, which likely reduced the severity of the thermal cycling effect. In future work, a heating unit will be incorporated to raise the sample surface temperature to room temperature or higher while exposed to air, thereby enabling more representative thermal cycling conditions.

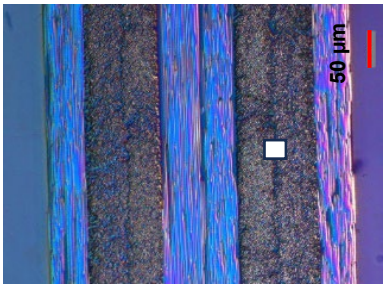

(a) Baseline, as-made (close-up location in white b)

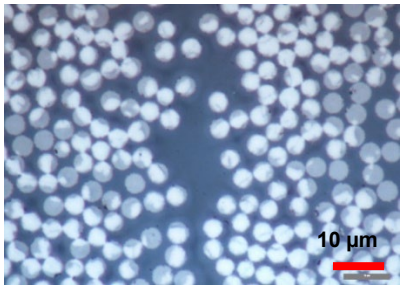

(b) Baseline, as-made

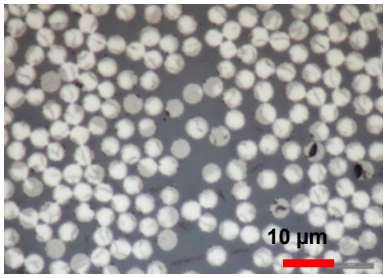

(c) Baseline, after 100 cycles

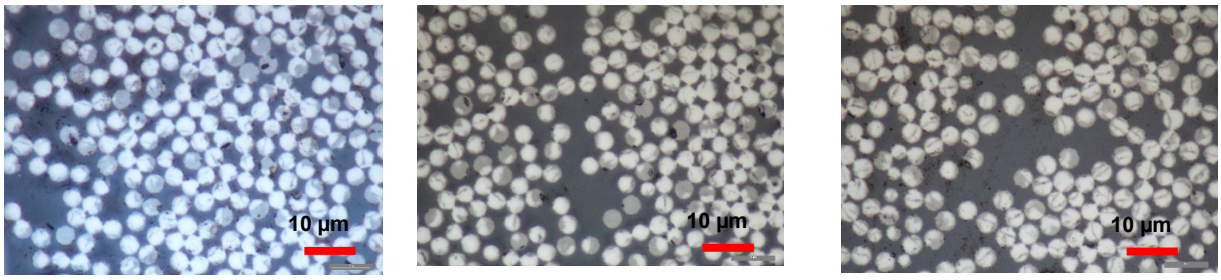

(d) Ultra-thin, 100 cycles (e) TP, after 100 cycles (f) TP-nano, after 100 cycles

Fig. 6: Microscopy images of cross-sections

4.3 Hydrogen permeation of composite materials

High pressure gas permeation tests were performed to measure specific permeation rates of various composite samples. The permeability characterization typically followed a three-step procedure. First, to minimize the effects of composite material outgassing, the test samples were pre-conditioned in a vacuum chamber for several days prior to permeation testing. The samples were tested in the apparatus using high-pressure nitrogen gas until the permeation rate stabilized. This baseline procedure may be repeated several times to reach stabilization. Once a steady-state permeation condition in nitrogen was achieved, high-pressure hydrogen permeation tests were performed.

During the permeation tests, the specimens were subjected to hydrogen at 86 psi on the upstream side, while the downstream side was maintained under vacuum. Each permeation test typically lasted approximately 24 hours, and up to eight tests were conducted on each sample under either nitrogen or hydrogen test conditions.

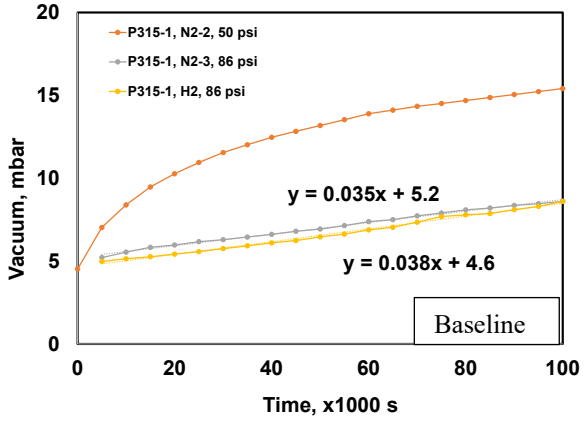

Fig. 7: Permeation results of as-made baseline composite laminate

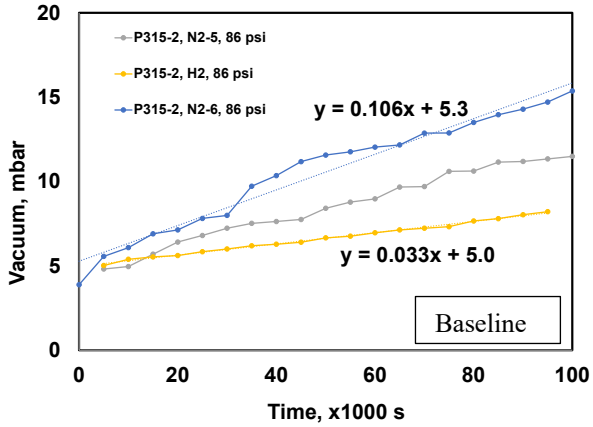

Fig. 8: Permeation results of baseline composite laminate after cryogenic thermal cycling

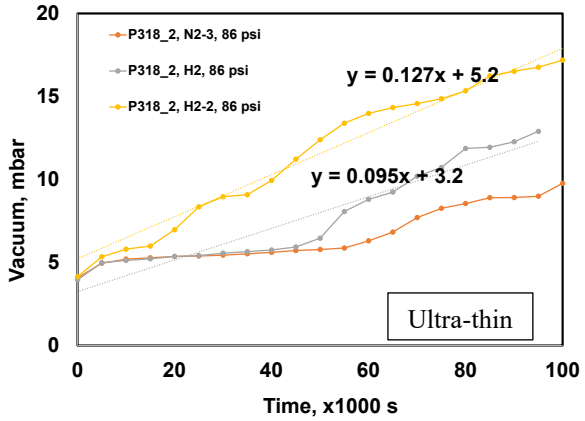

Fig. 9: Permeation results of composite laminate with ultra-thin ply after cryogenic thermal cycling

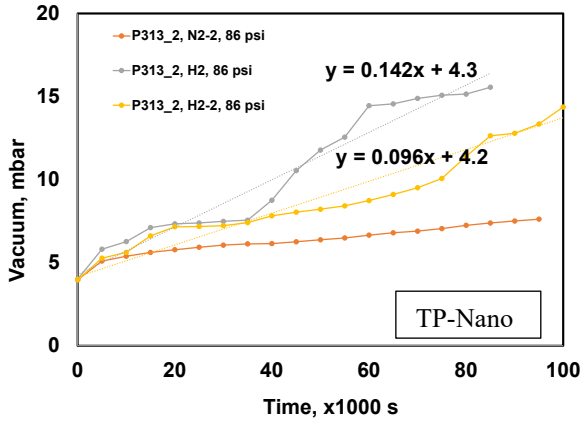

Fig. 10: Permeation results of composite laminate with TP-nano coating after cryogenic thermal cycling

Permeation tests were conducted on the as-manufactured baseline composite samples as well as on composite samples after cryogenic conditioning. The experimental results show the change in downstream vacuum pressure over time while the specimens were exposed to a constant upstream hydrogen pressure of 85 psi, as illustrated in Fig. 7 - Fig. 10. The slope of each curve is linked to the hydrogen permeation rate through the test samples.

As compared with the baseline sample, which exhibited a pressure change rate of 0.038 mbar/s, cryogenic exposure (see Fig. 8) did not cause a significant change in the baseline composite, with a measured pressure change rate of 0.033 mbar/s. However, samples containing either an ultra-thin ply or a TP-nano barrier showed a noticeable increase in the rate of pressure change, indicating reduced resistance to hydrogen permeation. Pressure change rates in the range of 0.095–0.142 mbar/s were measured for these samples, as shown in Fig. 9 and Fig. 10.

It is also noteworthy that the baseline samples, both with and without cryogenic exposure, exhibited a nearly linear pressure increase over time. In contrast, noticeable fluctuations in the pressure change rate were observed for samples containing barrier layers. Repeated tests confirmed that the permeation rates of these modified samples remained higher than those of the baseline samples. A summary of the calculated permeability coefficients, as defined in Eqn. 2 is provided in Table 2. Overall, the permeability of the modified composite samples increased by approximately two to four times compared with the unmodified baseline composite. However, since no microcracking was observed in any of the samples during microscopic examination, the measured permeability values require further validation to confirm the observed trends.

Table 2: Summary of permeability rates of composite samples

Permeability coefficient (barrer)	Baseline, as made	Baseline, 100 cycles	Ultra-thin, 100 cycles	TP-nano, 100 cycles
Hydrogen Test #1	169.0	146.8	345.3	674.4
Hydrogen Test #2			461.7	455.9

4.4 Implications of hydrogen permeation on tank design

An estimation was performed to evaluate the daily hydrogen leak rate of a storage tank made from the baseline composite material, using the measured permeability of 169 barrers. In this estimation, a liquid hydrogen tank with a total length of 5 m and a diameter of 1 m was considered, with a wall thickness of 20 mm. For simplicity, the tank ends were assumed to consist of two hemispherical domes. A pressure differential of 100 psi across the tank wall was assumed. Based on these assumptions, the tank would contain approximately 207 kg of liquid hydrogen when filled to 80 percent of its total volume. Using the measured permeability of the baseline composite material, the estimated hydrogen permeation loss was calculated to be about 5.35 g of hydrogen per day, corresponding to approximately 0.0026 percent of the stored hydrogen per day. The hydrogen loss for the TP-nano sample, which has the worst permeability rate of 674 barrers after 100 cycles of cryogenic exposure, is approximately 21.4 g/day.

According to SAE J2579 [13], the maximum allowable hydrogen permeation rate for onboard hydrogen storage systems in vehicles is 46 Ncm³ per hour per litre of tank volume. For the tank volume of 3.67 m³ (3670 L) considered in this estimation, the allowable permeation rate would be approximately 364 g of hydrogen per day for the entire tank. This estimation indicates that a tank constructed from the composite material evaluated in this study would readily meet the permeation limits specified in SAE J2579.

5. Summary

This study investigates the potential benefits of hydrogen barrier materials in improving hydrogen permeation resistance of composite materials, with consideration of cryogenic thermal cycling effects. The work led to the development of a cryogenic cyclic conditioning facility and a composite permeation testing apparatus at the National Research Council of Canada. The study also examined the possible formation of microcracking in composite materials as a result of repeated exposure to liquid nitrogen. In addition, the development and integration of hydrogen barrier layers were explored. Ultra-thin ply and nanomaterial-modified thermoplastic hydrogen barriers were incorporated into the composite laminates, and their effects on hydrogen permeability were evaluated.

Preliminary results show that the investigated composite material, an out-of-autoclave curable system, exhibits excellent resistance to microcracking after 100 cycles of thermal cycling in liquid nitrogen. This observation is consistent with the similar permeability rates measured for samples tested before and after cryogenic exposure. However, unexpected results were obtained for the samples containing hydrogen barrier layers. The incorporation of ultra-thin ply or nanomaterial-modified thermoplastic barriers appeared to result in higher permeability rates compared with the baseline composite, although no microcracking was observed in any samples subjected to cryogenic cycling. As the permeation measurement facility is still in the commissioning stage, further investigation is required to validate these findings.

Overall, the estimated hydrogen leak rate of the studied composite material is very low, based on the measured permeability rate. The estimate suggest that a hydrogen tank fabricated from the composite material evaluated in this study would readily meet the permeation limits specified in

SAE J2579 for onboard hydrogen storage. Further work is required to ensure accuracy of the measurements of permeability coefficient of composite samples.

Acknowledgement

The authors acknowledge the technical support of Richard Desnoyers, Sandi Robertson, Derek Winfield, Martin Tanguay, Ian Chevrette, Kulbir Birdi, and other technical staff at the National Research Council of Canada for their assistance with sample fabrication, testing, and microscopy.

References

[1] *Energy Efficiency 2025 Market Report*, International Energy Agency. Transport. Paris, IEA; 2025.

[2] Turner J., Contaut S., Tarantino A., Masson A., *Cryogenic Hydrogen Fuel System and Storage Roadmap Report. 2022*, Fly Zero, Aerospace Technology Institute.

[3] Johnson T. F., Sleight D.W., and Martin R.A., *Structures and Design Phase I Summary for the NASA Composite Cryotank Technology Demonstration Project*, The American Institute of Aeronautics and Astronautics (AIAA) SciTech 2013 Forum, Maryland, USA, 2013.

[4] Okonkwo P. C., Barhoumi E. M., Belgacem I. B., Mansir I. B., Aliyu M., Emori W., Uzoma P. C., Beitelmal W. H., Akyuz E., Radwan A. B., Shakoor R.A., *A focused review of the hydrogen storage tank embrittlement mechanism process*, International Journal of Hydrogen Energy, 48 (2023) 12935-12948

[5] Park, J., Kim, S., & Lee, H. *Permeation Behaviour of Hydrogen in Carbon Fibre Composites under Cryogenic Conditions. International Journal of Hydrogen Energy*, Vol. 44, No. 12, 2019.

[6] Kubo, S., Okubo, K., & Fujii, T.. Characteristic behaviors of CFRP and GFRP at cryogenic temperature under static and cyclic loadings. WIT Transactions on The Built Environment, 85, 2006

[7] Aoki T, Ishikawa T, Kumazawa H, Morino Y. *Cryogenic mechanical properties of CF/polymer for tanks of reusable rockets*, Adv Compos Mater 2001;10:349–56.

[8] Kumazawa H, Aoki T, Susuki I, *Analysis and experiment of gas leakage through composite laminates for propellant tanks*, AIAA J, 2003;41:2037–44.

[9] Galos J., *Thin-ply composite laminates: a review*. Composite Structures 236 (2020): 111920.

[10] Ioannis Katsivalis, Virginia Signorini, Fredrik Ohlsson, Christoph Langhammer, Matteo Minelli, Leif E. Asp, *Hydrogen permeability of thin-ply composites after mechanical loading*, Composites: Part A 176 (2024) 107.

[11] Wang, J., et al. *Incorporation of silica network and modified graphene oxide into epoxy coating for enhanced anticorrosion performance*. *Journal of Applied Polymer Science*, vol. 137, no. 49, 2020, p. 49405. DOI: 10.1002/app.49405.

[12] ASTM D1434-23, *Standard Test Method for Determining Gas Permeability Characteristics of Plastic Film and Sheeting*. ASTM International, USA.

[13] SAE J2579: *Standard for Fuel Systems in Fuel Cell and Other Hydrogen Vehicles*, SAE International, 2023.